View Article Online
View Journal

Green Chemistry

Cutting-edge research for a greener sustainable future

Accepted Manuscript

This article can be cited before page numbers have been issued, to do this please use: L. Zhang, R. Bu, X. Liu, P. Mu and E. Gao, *Green Chem.*, 2021, DOI: 10.1039/D1GC02118D.

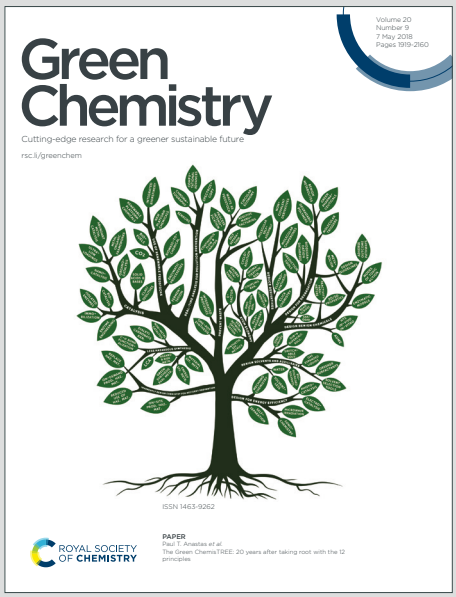

ROYAL SOCIETY OF CHEMISTRY

rsc.li/greenchem

View Article Online
DOI: 10.1039/D1GC02118D

ARTICLE

Schiff-base molecules and COFs as metal-free catalysts or silver supports for carboxylation of alkynes with CO_2

Received 00th January 20xx,
Accepted 00th January 20xx

DOI: 10.1039/x0xx00000x

Lin Zhang,[a] Ran Bu,[a] Xiao-Yan Liu,[a] Peng-Fei Mu[a] and En-Qing Gao*[a]

Carboxylating terminal alkynes with CO_2 to produce propiolic acids is an atom-economic and high-value route for CO_2 fixation and utilization, but the conversion under mild conditions needs transition metal catalysts. In this article, we demonstrated for the first time the transition-metal-free organocatalysts for the reaction. The efficient catalysts are the Schiff bases derived from 1,3,5-triformylphloroglucinol (Tp), either homogeneous (discrete molecules) or heterogeneous (covalent organic frameworks, COFs). The key catalytic sites are the phenoxo and imine groups, which activate CO_2 through phenoxo-CO_2 complexation and also activate the C(sp)-H bond through bifurcate C-H···N_{imine} and C-H···$O_{phenoxo}$ hydrogen bonds. The 2,2'-bipyridyl sites in the COF also contribute to the catalytic performance. The COF catalyst is less active than the molecular one but has the advantages of heterogeneous catalysis. Higher performance was also demonstrated by combining silver nanoparticles (AgNPs) with the intrinsically catalytic COF. This work opens up the potentials of developing transition-metal-free catalysts for the CO_2 conversion reaction and demonstrates the new prospects of COFs as tailorable platforms for heterogeneous catalysis.

Introduction

CO_2 is the chief culprit of the greenhouse effect and also a valuable single-carbon (C1) source for its ubiquity, renewability, nontoxicity and cheapness.[1, 2] Therefore, the use of CO_2 for green and economical organic synthesis has attracted continuous interest in the community of sustainable chemistry.[3-5] In this context, various C-C, C-N and C-O coupling reactions of CO_2 fixation have been developed in recent years.[6-8] Here we are focused on the carboxylation of terminal alkynes with CO_2. The reaction provides a straightforward atom-economic route to propiolic acids, which are valuable feedstocks for chemical and pharmaceutical industries.[9-11]

A general difficulty in CO_2 conversion is its intrinsic inactivity arising from the high thermodynamic stability and kinetic inertness.[12, 13] Classical carboxylation reactions with CO_2 make use of highly reactive and stoichiometric nucleophiles (bases) such as organolithium or Grignard reagents to deprotonate alkynes (Scheme 1a, route A).[14, 15] The methods have a poor compatibility with functional groups and require harsh conditions (anhydrous, anaerobic and so on), which offset the benefits of CO_2. Carboxylation of terminal alkynes can proceed smoothly in the presence of excess weak bases like Cs_2CO_3,[16] DBU (1,8-Diazabicyclo[5.4.0]undec-7-ene)[17] and TBD (1,5,7-triazabicyclo[4.4.0]dec-1-ene),[18] but high temperature and high CO_2 pressure are needed (Scheme 1a, route B). To overcome these troublesome problems, current research has been devoted to the development of efficient catalytic systems. The catalysts thus far reported for direct C-H carboxylation of terminal alkynes are transition-metal catalysts, mostly silver and copper (Scheme 1a, route D).[19-21] The catalysis involves the base-assisted formation of metal acetylide intermediate and subsequent CO_2 insertion to the M-C bond.[22, 23] The catalytic transformation can occur under more friendly and less energy-consuming conditions with improved group tolerance. For

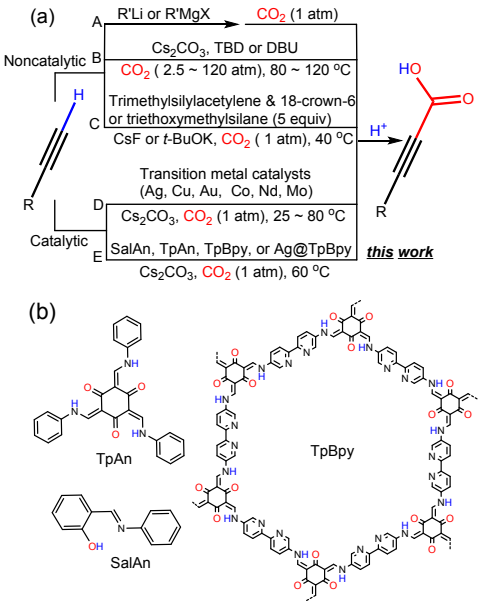

Scheme 1 (a) Routes for the carboxylation of terminal alkynes with CO_2. (b) The Schiff-base molecules and COF catalysts used in this article.

[b.] *Shanghai Key Laboratory of Green Chemistry and Chemical Processes, School of Chemistry and Molecular Engineering, East China Normal University, Shanghai 200062, China. E-mail: eqgao@chem.ecun.edu.cn*

†Electronic supplementary information (ESI) available: Experimental and characterization data. See DOI: 10.1039/x0xx00000x

View Article Online
DOI: 10.1039/D1GC02319D

simpler operation and better economy, recyclable heterogeneous catalysts have been obtained by loading Ag, Cu and Au species (mostly silver nanoparticles, AgNPs) on various matrices such as inorganic oxides, organic polymers, carbon nitride and metal-organic frameworks (MOFs).[24-27] However, the use of transition metals also causes practical problems such as complicated preparation, high cost, toxic metal leaching and contamination. Therefore, transition-metal-free reactions under mild conditions are desired. In this respects, two alkynylsilane-mediated carboxylation approaches have been reported (Scheme 1a, route C), which involve two sequential base-promoted (CsF or t-BuOK) reactions: silylation of terminal alkynes and CO_2 insertion into the Si-C bonds.[28, 29] However, approaches significantly reduce the atom economy and enhance the cost of the excess use and unrecoverable consumption of silylating reagents in these of production and waste disposal. Obviously, the more environmentally benign and cost-effective protocols lie in the use of transition-metal-free catalysts or organocatalysts, preferably heterogeneous. To our knowledge, however, such catalysts for direct carboxylation of alkynes remain undeveloped.

Covalent organic frameworks (COFs) are crystalline organic porous materials constructed from modular building blocks with specific functionalities that afford dynamic and self-regulating covalent assembly.[30, 31] Since the first report by Yaghi et al. in 2005,[32] the study of COFs has rapidly grown into a multidisciplinary field and provided versatile materials platforms for many potential applications.[33-35] In particular, the inherent advantages make COFs intriguing for applications in heterogeneous catalysis. They can exhibit excellent chemical stability.[36] The ordered structure allows uniform dispersion of functional sites for the benefit of catalytic efficiency.[37] The permanent porosity and high surface area permit rapid mass transport of substrates/products and high accessibility of functional sites.[38] The modular and tailorable structure can be modified at the molecular level through reasonable strategies to achieve new or better catalytic performance.[39] COF-based heterogeneous catalysis can be achieved by (i) utilizing the active sites at the frameworks, either intrinsic or elaborately incorporated, and (ii) using the porous organic matrices to support metal nanoparticles or other catalytic species.[40] A number of COFs have been used for catalytic CO_2 conversion, mainly including photo-/electrocatalytic reduction and cycloaddition with epoxides.[41-43] There have been only a few studies of alkyne-CO_2 carboxylation using COF-supported metal catalysts.[44, 45]

Our previous study suggested that Cu(I)-modified COFs can promote the carboxylation reaction with concomitant Cu(I)-to-Cu(II) oxidation and that the catalysts can be regenerated by reduction with KI.[46] Here, we report the extension of the study to COF-supported AgNPs (Ag@TpBpy, Scheme 1a, route E), which are more efficient and more facile to regenerate. More interestingly, we demonstrate that the pristine imine-linked organic framework and the corresponding discrete Schiff-base molecules can intrinsically catalyse the carboxylation reactions. By comprehensive comparative studies, we reveal that the key active sites in the pure organic catalysts are the phenolato and imine groups, which cooperate to activate the C(sp)-H bond and CO_2. The results pay the way for the development of transition-metal-free catalysis for the CO_2-alkyne reaction, either homogeneous or heterogeneous.

Results and discussion

Synthesis and characterization

TpBpy was synthesized from 2,2'-bipyridine-5,5'-diamine (Bpyda) and 1,3,5-triformylphloroglucinol (Tp), using a previously reported mechanochemical method[47] with some modification. Ag@TpBpy was obtained by impregnation of TpBpy with $AgNO_3$ solution and subsequent reduction with hydrazine.

The as-synthesized TpBpy exhibits the X-ray diffraction (XRD) profile characteristic of the crystalline 2D hexagonal COFs (Fig. 1a). Pawley refinements of the XRD pattern produced a good agreement with the eclipsed AA stacking of 2D hexagonal layers in the *P6/m* space group with a = 29.3 Å and c = 3.5 Å. The theoretical channel size is about 2.5 nm (H···H distance between opposite edges of the hexagonal window). The π–π stacking distance between the COF layers is 3.5 Å using the d spacing between the (001) planes (2θ = 26.7 ± 2°). As can be seen from Fig. 1b, the crystalline framework retains its integrity after impregnation with $AgNO_3$ and subsequent reduction. After reduction, the characteristic (111) and (200) diffraction peaks of metallic Ag appear at 2θ = 38° and 44.2°, respectively, indicating the successful immobilization of AgNPs.[48]

In the FT-IR spectrum of TpBpy (Fig. 1c), there are no bands characteristic of the NH_2 group (3205 and 3313 cm^{-1}) for Bpyda and the formyl C=O vibration (1644 cm^{-1}) of Tp, indicating the occurrence of imine condensation. The peaks at 1570 and 1442 cm^{-1} are attributable to the skeleton C=C and C=N stretching vibrations of the pyridyl and benzene rings of the COF. The strong absorption observed at 1604 cm^{-1} is generally ascribed to ν(C=O) of the Tp-based COFs in the keto-enamine tautomeric form. These results confirmed the successful preparation of TpBpy as proposed. The IR spectrum after AgNPs loading is overall similar (Fig. 1d). However, a shoulder absorption can be discerned at the low-wavenumber side of the 1570 cm^{-1} band, and the relative intensity of the 1570 cm^{-1} band to the 1604 cm^{-1} band is reversed. Always observed for different batches of Ag-loaded COFs, these changes in IR spectra could be indicative of the interactions between AgNPs and the organic support.

The elemental composition and states were investigated using X-ray photoelectron spectroscopy (XPS) (Fig. S1, in the ESI). The N 1s XPS spectrum of TpBpy (Fig. 1e) shows two peaks at 399.9 eV and 398.7 eV, corresponding to secondary amine and pyridyl nitrogens, respectively. After immobilization of AgNPs, the N 1s profile changes, and the deconvolution reveals a new peak at 399.3 eV, which could be due to the interaction between Ag and N. The success of Ag loading is confirmed by the presence of the XPS signals of Ag, and the gap (6.0 eV) between the $3d_{3/2}$ (374.0 eV) and $3d_{5/2}$ (368.0 eV) is characteristic of metallic Ag(0) (Fig. 1f).[48] The small bathochromic shift of the binding energy compared with the

View Article Online
DOI: 10.1039/D1GC02118D

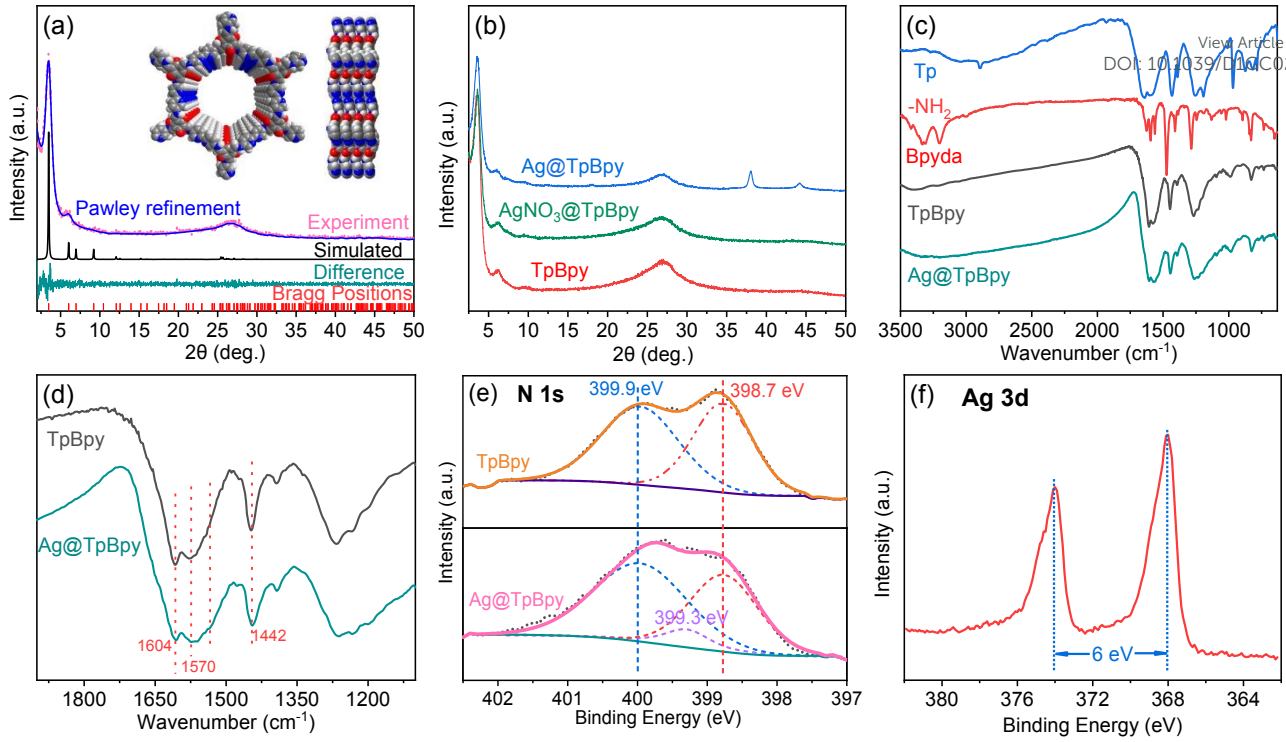

Fig.1 (a) Experimental and simulated XRD patterns of TpBpy. The Pawley refinement is also provided (R_p=4.96%, R_{wp}=7.07%). (b) XRD patterns of TpBpy, $AgNO_3$@TpBpy and Ag@TpBpy. (c) FT-IR spectra of the precursors, TpBpy and Ag@TpBpy. (d) Magnified FT-IR spectra of TpBpy and Ag@TpBpy (e) N 1s XPS spectra of TpBpy and Ag@TpBpy. (f) Ag 3d XPS spectra for Ag@TpBpy.

reported value for Ag(0) ($3d_{5/2}$ = 368.3 eV)[49] could indicate weak interactions between AgNPs and organic ingredients.

The scanning electron microscope (SEM) image of TpBpy indicates an irregular morphology (Fig. 2a). There is no change in the morphology from the SEM images after metal modification (Fig. 2b). The high-resolution transmission electron microscope (HRTEM) images of AgNPs@TpBpy (Fig. 1c and 1d) show that AgNPs were well dispersed in the substrate with particle sizes 3 - 6 nm. The lattice fringes of metallic Ag are clear, with the interplanar spacing of 0.23 and 0.20 nm corresponding to the (111) and (200) planes, respectively. It is impossible that the relatively large AgNPs are enclosed within the channels or intercalated between layers in a COF crystallite. It is most likely that the *post-synthetically* introduced AgNPs are

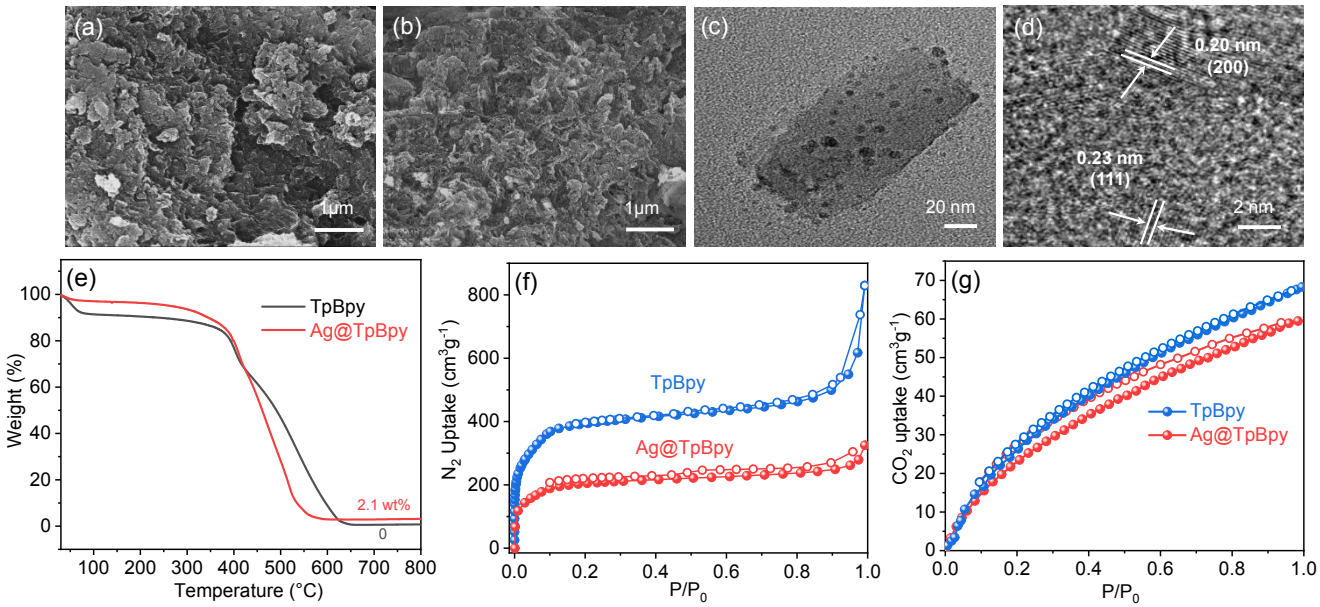

Fig.2 (a-d) Microscopic images of TpBpy (a, SEM) and Ag@TpBpy (b, SEM; c and d, TEM). (e) TGA of TpBpy and Ag@TpBpy. (f) N_2 absorption-desorption isotherms collected at 77 K. (g) CO_2 sorption isotherms at 273 K.

View Article Online
DOI: 10.1039/D1GC02118D

located at the surfaces of crystallites and/or between the COF crystallites.[50]

Thermogravimetric analysis (TGA) indicates high thermal stability (up to 400 °C) for both TpBpy and Ag@TpBpy. (Fig. 2e). The pure organic framework decomposes completely without any residue above 640 °C. Differently, perhaps owing to an Ag-catalysed process, the decomposition of the framework in Ag@TpBpy is more rapid and gives a constant-weight residue above 560°C (2.1 wt%). The residue should be elemental silver, the amount being in good agreement with the Ag content (1.9 wt%) measured by inductively coupled plasma atomic emission spectrometer (ICP-AES).

N_2 adsorption measurements at 77 K were performed with both TpBpy and Ag@TpBpy (Fig.2f). The COF exhibits a type-I adsorption isotherm, and the Brunauer–Emmett–Teller (BET) surface area is 1480 m^2 g^{-1}. Ag@TpBpy also shows a type-I adsorption isotherm, verifying the retention of the microporosity. The BET surface area is reduced to 761 m^2 g^{-1} after Ag loading, which is due to pore blocking by AgNPs. CO_2 adsorption was tested at 273K and 298K (Fig. 2g and Fig. S2a, ESI). TpBpy displays an adsorption capacity of 68.3 cm^3 g^{-1} for CO_2 at 273 K and ambient pressure. The capacity decreases to 59.4 cm^3 g^{-1} for the AgNPs-loaded COF. The adsorption heat calculated using the Clausius-Clapeyron equation at low CO_2 pressure is 27.7 kJ mol^{-1} for TpBpy and 33.0 kJ mol^{-1} for Ag@TpBpy (Fig. S2b in the ESI). The increased adsorption heat suggests the higher affinity of AgNPs for CO_2 molecules.

For comparative catalytic studies, a series of similar COFs and the corresponding Ag@COFs were synthesized by similar methods, where the 2,2'-bipyridyl or hydroxyl groups in TpBpy were replaced by biphenyl or methoxyl, respectively (Scheme 2). The characterization data are provided in the ESI (Fig. S3). It is notable that impregnation of TpBD with $AgNO_3$ directly led to Ag@TpBD without any reduction procedure (Fig. S3a). The spontaneous reduction from Ag(I) to Ag(0) has been observed for the imine-based COF derived from 1,3,5-benzenetricarbaldehyde and *p*-phenylenediamine,[51] where the residual amine groups at the edges of the COF was assumed to be the reductant. The reductive Ag(I) incorporation observed for TpBD could arise from a similar mechanism. The spontaneous reduction was also observed for impregnation of TpOMeBD with $AgNO_3$, but no Ag(I) reduction was observed for all of the three COFs derived from Bpyda (Fig. S3 and Fig. 1b). Therefore, the reductivity of imine-based COFs is dependent upon the diamine linkers used. A possible reason is that the Ag(I) state is stabilized by its coordination with the N,N'-chelating bipyridyl linker.

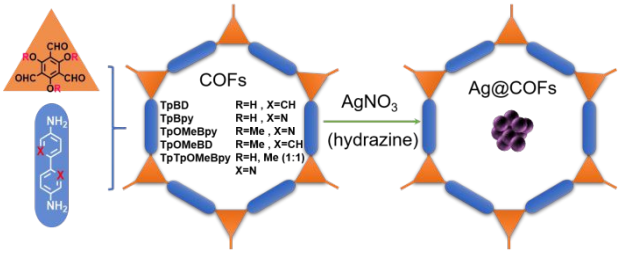

Scheme 2 Various COFs and Ag@COFs synthesized in this work.

Catalysis with Ag@COF

The carboxylation of phenylacetylene with CO_2 under the atmospheric pressure was selected as model reaction for catalytic tests. The results of the control tests with various catalysts or under different conditions are summarized in Table 1. Previous studies have established that N,N-dimethylformamide (DMF) and dimethylsulfoxide (DMSO) are the favourable solvents for the catalytic reaction (ESI, Table S2). According to entries 1 and 2 in Table 1, Ag@TpBpy performs much better in DMSO (yield 93% after 6 h in the presence of Cs_2CO_3 at 60 °C) than in DMF (62%). Therefore, DMSO was chosen for further tests. The control reaction in the presence of Cs_2CO_3 but in the absence of the catalyst proceeded slowly with a yield of 30% under the same conditions (Entry 3). The reaction without Cs_2CO_3 gave no conversion, no matter whether Ag@TpBpy was used or not (Entries 4 and 5). The results confirm the crucial role of Cs_2CO_3 and the catalytic activity of Ag@TpBpy. The reaction over Ag@TpBpy is significantly more efficient than that over pure TpBpy (Entries 1 and 6), clearly indicating that AgNPs play an important catalytic role. Comparing the reactions with and without TpBpy (Entries 3 and 6) suggests the COF itself is also active, which is to be discussed later. Here we focus on the effect of the matrices on the performance of Ag@COFs. A series of isoreticular and iso-dimensional COF matrices were used to support AgNPs (Scheme 2). First, the hydroxyl groups in TpBpy were partially or completely changed to methoxyl. The resultant Ag catalysts, Ag@TpTpOMeBpy (Ag content 3.2 wt%) and Ag@TpOMeBpy

Table 1 Catalytic data for carboxylation of phenylacetylene with CO_2.[a]

Entry	Catalyst	Base	Time (h)	Yield[d] (%)
1	Ag@TpBpy	Cs_2CO_3	6	93
2[b]	Ag@TpBpy	Cs_2CO_3	6	62
3	-	Cs_2CO_3	6	30
4	-	-	6	-
5	Ag@TpBpy	-	6	-
6	TpBpy	Cs_2CO_3	6	67
7	Ag@TpTpOMeBpy	Cs_2CO_3	12	86
8	Ag@TpOMeBpy	Cs_2CO_3	12	64
9	Ag@TpBD	Cs_2CO_3	6	66
10[c]	Ag@TpBD	Cs_2CO_3	6	80

[a] Reaction condition: phenylacetylene (0.5 mmol), Cs_2CO_3 (1.5 mmol), CO_2 (balloon), catalysts (20 mg, unless otherwise specified), 60 °C, DMSO (3 mL). [b] The solvent is DMF (3 ml) instead of DMSO. [c] Ag@TpBD (76 mg), the Ag amount is equal to that for Ag@TpBpy (20 mg). [d] Yield of isolated product.

View Article Online
DOI: 10.1039/D1GC02118D

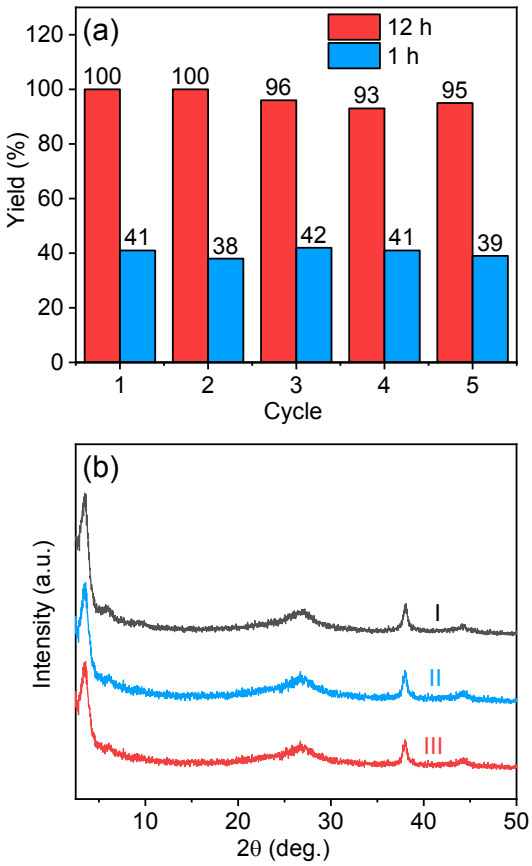

Fig. 3 (a) Recycling tests of the Ag@TpBpy catalyst (reaction conditions: phenylacetylene (0.5 mmol), Cs_2CO_3 (1.5 mmol), CO_2 (balloon), Ag@TpBpy (20 mg), DMSO (3 mL), 60 °C, 12 h or 1 h). (b) XRD patterns of the fresh catalyst (I) and those after 5 catalytic runs, the reaction time being 1 h (II) or 12 h (III).

(4.2 wt%), have higher Ag content than Ag@TpBpy (1.9 wt%). However, the carboxylation reactions using the methoxyl-containing catalysts gave significantly lower yields even though the reaction time was doubled (Entries 7 and 8). Significant yield decrease was also observed for Ag@TpBD (Ag content 0.5 wt%) (Entries 9 and 10), in which the COF has biphenyl linkers in the place of bipyridyl. Therefore, the catalytic activity is strongly affected by the COF matrix that supports AgNPs. Ag@TpBpy is the best catalyst, which could be simply because its activity arises not only from the metal site but also from the organic matrix (*vide infra*).

The recyclability of Ag@TpBpy was studied (Fig. 3a). The catalyst isolated from a catalytic run was directly used for the next run after simple washing and drying. When each run was performed for 1 h, the yields for 5 consecutive runs were kept around 40±2 %, suggesting no degradation in intrinsic activity. When the reaction time was increased to 12 h for each run, complete or nearly complete conversions were observed for 5 runs. XRD measurements with the used catalysts confirm that the crystalline framework is retained (Fig. 3b). ICP-AES analysis indicates that the Ag content decreases from 1.9 to 1.5 wt% after 5 catalytic runs (12 h for each run), which accounts for the slight yield decrease observed for the long-time recycling experiments.

Table 2 Metal-free catalysis for carboxylation of phenylacetylene with CO_2.[a]

Entry	Catalyst	Yield (%)
1	None	30[b]/35[c]
2	TpBpy	67[b]/70[c]
3	TpBD	52[b]/57[c]
4	TpOMeBpy	48[b]
5	TpOMeBD	33[b]
6	TpAn	90[c]
7	SalAn	68[c]
8	PhAn	22[c]
9	phloroglucinol	37[c]
10	2,2′-bipyridine	27[c]

[a] Reaction conditions: phenylacetylene (0.5 mmol), Cs_2CO_3 (1.5 mmol), CO_2 (balloon), DMSO (3 mL), 60 °C, 6 h. The catalyst dosage was 20 mg for COFs and TpAn. Other catalysts were controlled to be equivalent to TpAn in amount of active sites. [b] Isolated yield. [c] Yield based on GC.

Transition-metal-free Catalysis

As mentioned above, the pure COF can catalyse the carboxylation reaction. Although the activity is lower than that of Ag@TpBpy, the finding is exciting because the transition-metal-free organocatalysts for the reaction are unprecedented. The finding is consistent with the fact that the COF matrices strongly affect the catalytic activities of Ag@COFs. These inspired us to further explore the transition-metal-free catalysis (Table 2). As can be seen, TpBD and TpOMeBpy also show intrinsic activity, which however is lower than that of TpBpy (Entries 3 and 4). The high intrinsic activity of TpBpy compared to other COFs could be responsible for its superiority as support for AgNPs (*vide supra*). Furthermore, the reaction over TpOMeBD gave a conversion comparable to that without any catalyst (Entry 5). The above results suggest that both phloroglucinol and bipyridyl moieties contribute to the intrinsic catalytic activity of TpBpy.

View Article Online
DOI: 10.1039/D1GC02118D

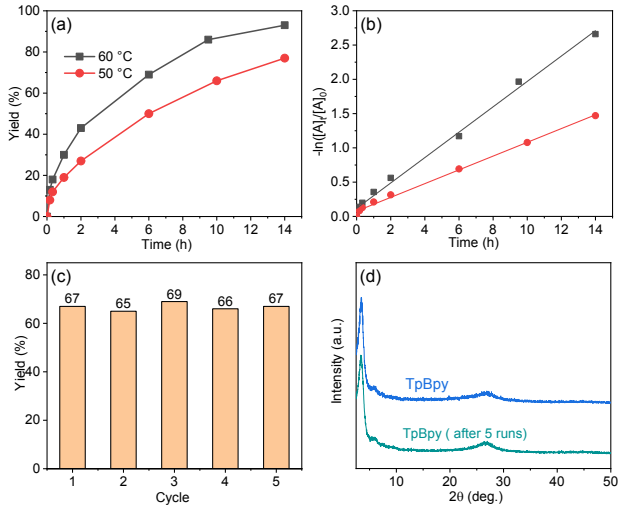

Fig. 4 (a) Kinetic plots for the carboxylation of phenylacetylene with CO_2. Conditions: phenylacetylene (0.5 mmol), CO_2 (1 atm, balloon), TpBpy (20 mg), Cs_2CO_3 (1.5 mmol), DMSO (3 mL). (b) The fit of the data in (a) to the first-order kinetics. (c) Recycling tests under the aforementioned conditions (60 °C, 6 h for each run). (d) XRD patterns of the fresh and used catalysts.

Table 3 Carboxylation of terminal alkynes catalysed by TpBpy.[a]

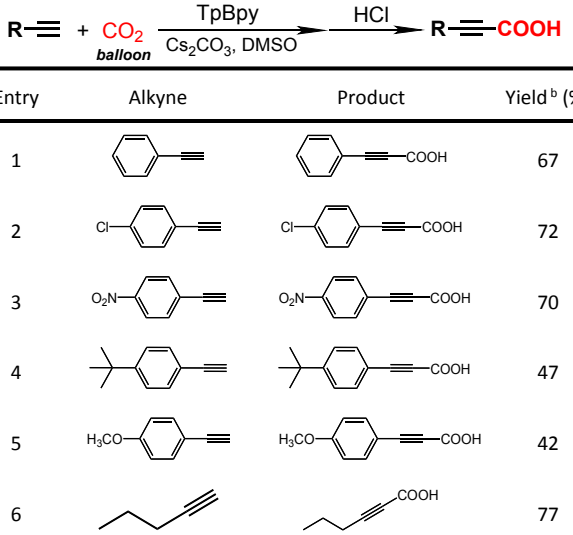

[a] Reaction conditions: terminal alkynes (0.5 mmol), TpBpy (20 mg), Cs_2CO_3 (1.5 mmol), CO_2 (balloon), DMSO (3 mL), 60 °C, 6 h. [b] Yield of isolated product.

To further determine the effective catalytic sites in TpBpy, we performed control experiments with several model molecules that contain specific functional sites similar to those in the COF. The vertex structure of TpBpy is modelled by the Schiff base (TpAn) derived from Tp and aniline (An). The control catalytic test suggests that TpAn has more prominent activity than TpBpy for the CO_2 insertion reaction. The model monomer affords a high yield of 90% (Entry 6), which is comparable to that achieved with Ag@TpBpy under identical conditions. The simpler model phenol-imine molecule (SalAn) derived from salicylaldehyde and aniline also significantly catalyses the reaction. With the catalyst dosage being controlled to be equivalent in hydroxyl and imine amount, the yield of the reaction using SalAn is obviously lower than that with TpAn (Entry 7). This suggests that the tri(enol-imine) core of TpAn is more efficient than the discrete enol-imine structure of SalAn. Further tests were performed with the imine molecule (PhAn) derived from phenyl aldehyde and aniline, lacking the phenolic hydroxyl group. PhAn shows no catalytic effect and even has some inhibitory effect as compared to the reaction with Cs_2CO_3 alone (Entry 8). On the other hand, phloroglucinol shows a very weak promoting effect (Entry 9). The comparison suggests that the phenolic and imine sites cannot efficiently promote the CO_2 insertion reaction when standing alone, but they cooperate in the enol-imine structure to afford a prominent catalytic activity. The yield of the catalytic reaction with 2,2'-bipyridine is similar to that without it, so 2,2'-bipyridine alone is inactive (Entry 10). However, the comparisons between TpBpy and TpBD and between TpOMeBpy and TpOMeBD suggest that the 2,2'-bipyridyl moieties in the COFs does contribute to the catalytic reaction. This reflects that the heterogeneous catalytic process in the confined space of the porous solid is different from the homogeneous one. Therefore, the catalytic activity of TpBpy mainly arises from the enol-imine group at the corner of the hexagonal channel. The discrete Schiff-base counterpart TpAn shows a higher activity, but TpBpy is superior to TpAn with respect to operational faciliness and environmental friendliness because the COF is insoluble and permits heterogeneous catalysis.

Our further studies were focused on TpBpy. The solvent and base effects on the metal-free catalyst were investigated (Table S1). The catalytic reaction in presence of Cs_2CO_3 can also proceed in DMF and propylene carbonate (PC), but the conversion is significantly slower than that in DMSO. Only minor conversion was observed for the reaction with acetonitrile or dioxane as solvent. Therefore, DMSO is the optimal solvent for TpBpy. No product was detected for the catalytic reaction in the presence of other bases, including Na_2CO_3, K_2CO_3, KOH or triethylamine (Entries 6-9, Table S1). The observation indicates the uniqueness of Cs_2CO_3 for the reaction. Not only does it serve to provide the basic condition, but the Cs^+ cation also plays a crucial role in the catalytic process, irreplaceable by Na^+ and K^+. Kinetic studies for the catalytic carboxylation reaction of phenylacetylene were carried out at 50 and 60 °C in DMSO-d_6. The yield was analysed at given time intervals using ^{1}H NMR. The yield at 60 °C reached 95 % in 14 h (Fig. 4a). The metal-free heterogeneous catalytic efficiency is even higher than many Ag and Cu catalysts,[44, 52] which often need a longer time to reach a conversion above 90%. Decreasing the reaction temperature by 10 °C leads to a significant reduction in yield (76 %). As demonstrated in Fig. 4b, the conversions at both temperatures follow the first-order kinetics with reaction rate constants of 0.00164 and 0.00304 s^{-1} for 50 and 60 °C, respectively ($R^2 > 0.99$ for the linear regression). The activation energy was calculated to be 51.3 kJ mol^{-1} according to the Arrhenius equation.

The substrate scope of the metal-free heterogeneous catalysis was examined. Under the mild conditions (60 °C, 1 atm CO_2 balloon), different terminal alkynes, including aliphatic and

View Article Online
DOI: 10.1039/D1GC02118D

aromatic ones, can smoothly undergo the CO_2 insertion reaction. The reactivity of different alkynes over the catalyst was checked by comparing the intermediate conversions at fixed reaction time. As can be seen from Table 3, the phenylacetylene derivatives with electron-withdrawing groups are more reactive than those with electron-donating groups. The substituent effects suggest that the reactivity is associated with the polarity or acidity of the terminal C-H bond: the electron-withdrawing substituents increase the polarity, and a higher polarity is beneficial to activation of the bond through hydrogen bonding.

As shown in Fig. 4c, the activity of the metal-free COF catalyst is fully retained in the 5 cycles tested. XRD measurements confirm that the crystalline framework remains unchanged after use (Fig. 4d). The results show the good recyclability of TpBpy, whose active sites are intrinsic to the framework and unleachable.

The catalytic performance of Ag@TpBpy and TpBpy are compared in Table S2 with that of previously reported Cu and Ag catalysts with various solid supports. Generally, Ag is superior to Cu in term of turnover frequency (TOF). Ag@TpBpy outperforms most previous Ag catalysts, including two previous COF-supported (Entries 8 and 9).[44, 45] Free of metal, TpBpy is superior to some supported Ag catalysts in term of mass efficiency, which we define as the amount of product yielded per unit of catalyst mass in unit time. Although TpBpy is still less efficient than most metal catalysts, our finding opens the possibility of metal-free catalysts for direct alkyne carboxylation.

Mechanism consideration

The catalytic mechanism of solid-supported Ag NPs for terminal alkyne carboxylation has been well established, including four main steps: (i) activation of the terminal C(sp)–H bond through π-complexation, (ii) simultaneous deprotonation and M–C(sp) bond formation, (iii) insertion of CO_2 to M–C(sp) to generate M-propiolate, and (iv) decomposition of M-propiolate to release propiolate and the catalytic metal center.[22, 23]

For the metal-free catalytic activity observed for TpBpy, TpAn and SalAn, we have demonstrated (*vide supra*) that the key is the combination of the phenol and imine groups in these structures. The phenol-imine combinational site may serve to activate both CO_2 and terminal alkynes. Considering the pK_a values, 8.8 for phloroglucinol[53] (9.9 for phenol[54]), 10.3 for HCO_3^-, and ~28.7 for phenylacetylene,[55] it is not easy for phenylacetylene to be deprotonated by Cs_2CO_3, but phloroglucinol or phenol can be deprotonated to form cesium

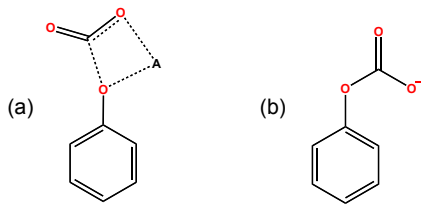

Scheme 3 Intermediates proposed for the Kolbe-Schmitt reaction (a, A = alkali metal) and for CO_2 capture by phenolate-based ionic liquids (b).

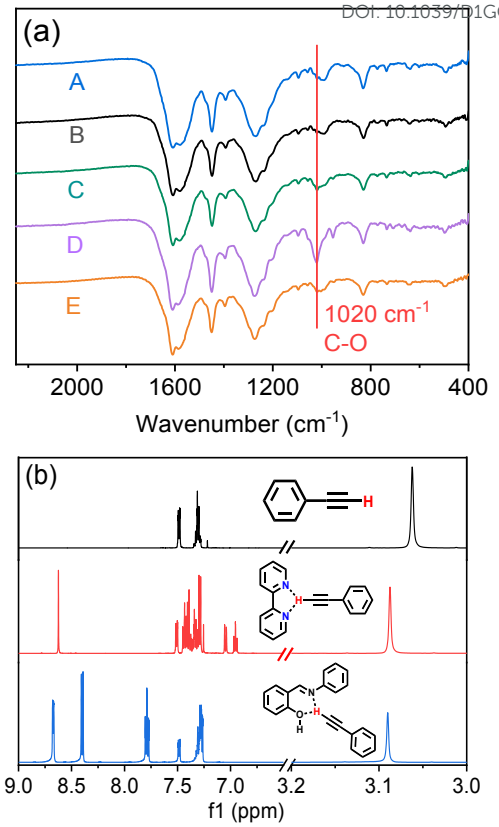

Fig.5 (a) FT-IR spectra of various samples of TpBpy. (A) as-prepared; (B) treated with CO_2; (C-E) samples after base treatment (Cs_2CO_3/DMSO), washing (DMSO and acetone) and drying (C), CO_2 treatment (D), and heating in vacuum (E). (b) ^{1}H NMR of phenylacetylene in $CDCl_3$ before and after addition of 2,2′-bipyridine and SalAn.

phenolates. This is reminiscent of the Kolbe-Schmitt reaction, a long-known carboxylation reaction for synthesis of hydroxybenzoic acids from alkali metal phenolates (PhOA, with A = alkali metal ion) and CO_2.[56] Experimental and computational studies support that CO_2 and PhOA form an intermediate PhOA-CO_2 complex at the first stage of the reaction (Scheme 3a).[57, 58] Similar phenoxo-CO_2 complexes have been proposed to be responsible for the reversible equimolar capture of CO_2 with phosphonium phenolate ionic liquids (Scheme 3b).[59] Accordingly, in the catalytic carboxylation of terminal alkynes, we can assume that CO_2 is activated by forming similar intermediate complexes with the phenoxo sites of the catalysts.

To probe the interactions of CO_2 with TpBpy, the COF was pre-treated with the saturated solution of Cs_2CO_3 in DMSO, thoroughly washed with DMSO and then stirred in CO_2 atmosphere for 30 min without any solvent. As shown in Fig. 5a, no appreciable change in IR spectra was observed after treatment with Cs_2CO_3 and washing, but the subsequent treatment with CO_2 led to a new IR peak appears at 1020 cm^{-1}, which disappeared after heating. The new IR absorption can be attributed to weak C-O bonds between CO_2 and phenoxo. In contrast, the COF without Cs_2CO_3 pretreatment does not show any IR changes after stirred in CO_2 atmosphere. Therefore, we can assume that the COF is deprotonated to generate phenoxo

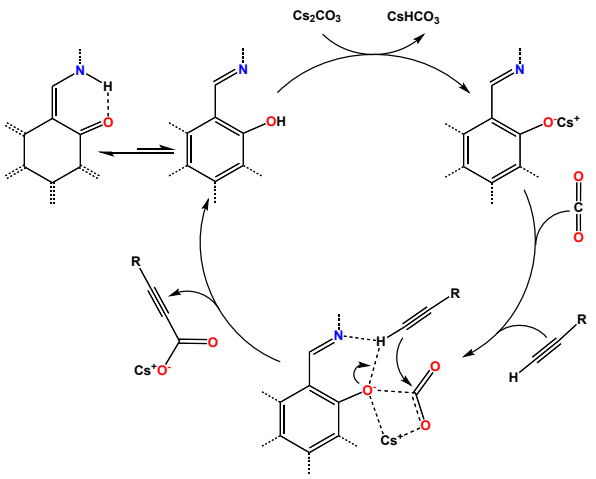

Scheme 4 The carboxylation reaction mechanism for the metal-free catalyst used in this study.

groups, which form PhO-CO_2 (or PhOCs-CO_2) complexes to activate CO_2. The presence of basic phenoxo groups is supported by the fact that soaking the Cs_2CO_3-treated and washing TpBpy in water leads to a basic solution (no pH change was observed in the control test with the pristine COF). Furthermore, CO_2 adsorption experiments reveal that the COF after Cs_2CO_3 treatment shows much higher adsorption heat at low CO_2 loading than the pristine COF (ESI, Fig. S4), which confirms greatly enhanced affinity to CO_2 owing to deprotonation.

On the other hand, the C(sp)-H group of terminal alkynes can form bifurcate hydrogen bonds with the chelating phenoxo-imine sites. The interaction was confirmed by ^{1}H NMR (Fig. 5b). The terminal H signal of phenylacetylene shifts from 3.062 to 3.090 ppm after the addition of SalAn, indicating the hydrogen bonding of C(sp)-H with the phenol-imine sites. We found that the imine linkage of SalAn is broken after treated with Cs_2CO_3, which prevents us from detecting the NMR change using deprotonated SalAn. However, the phenol group in TpBpy can be deprotonated without breaking the linkage. The deprotonated phenoxo-imine sites in the COF should be more prone to form hydrogen bonds.

On the basis of the above analysis, we proposed Scheme 4 for the metal-free catalytic mechanism through the phenol-imine sites. The key is the formation of the intermediate complex in which the C(sp)-H group is activated by chelating hydrogen bonding and CO_2 is activated by phenoxo. The intermediate complex can undergo proton transfer from C(sp)-H to phenoxo oxygen and simultaneous nucleophilic addition of alkynyl to activated CO_2, yielding the propiolate product and regenerating the phenol-imine sites. Additionally, the 2,2'-bipyridyl sites in TpBpy can provide an alternative approach for C(sp)-H activation. As shown in Fig. 5b, the ^{1}H NMR signal of C(sp)-H is shifted from 3.062 to 3.087 ppm upon adding 2,2'-bipyridine to the phenylacetylene/$CDCl_3$ solution, suggesting intermolecular interactions. Probably, the C(sp)-H group can form bifurcate hydrogen bonds with 2,2'-bipyridine.

Conclusions

View Article Online
DOI: 10.1039/D1GC02118D

Some new catalysts have been described for the catalytic carboxylation of terminal alkynes with CO_2. We found that the phenol-imine Schiff bases, either as discrete molecules or COFs, can efficiently promote the C-C coupling reaction. This is the first demonstration of transition-metal-free organocatalysts, either homogeneous or heterogeneous, for the reaction. The effective catalytic sites are the phenoxo and imine groups, which activate CO_2 through phenoxo-CO_2 complexation and also activate the C(sp)-H bond through hydrogen bonds. The molecular catalyst TpAn is more active than the COF catalyst TpBpy, but the latter has the advantages of heterogeneous catalysis and therefore is superior in sustainability. Combining both metal sites and organic sites, Ag@TpBpy affords an activity higher than the pure COF and comparable to the homogeneous organocatalyst, at the cost of using precious metals. This work provides optional catalysts for the CO_2-alkyne reaction and especially sheds new light on the developing of transition-metal-free catalysts for the reaction.

Experimental

Synthesis of TpBpy

342.4 mg (1.8 mmol) of *p*-toluene sulfonic acid monohydrate was thoroughly mixed was with Bpyda (83.8 mg, 0.45 mmol) in a mortar. Tp (63 mg, 0.3 mmol) was added and mixed adequately, and then 10 ~ 50 μL of water was added. The mixture was continuously ground until the formation of a dough. The dough was sealed in a glass vial and heated for 3 h at 120 °C. After cooling to room temperature, a deep reddish hard solid was obtained. The product was ground to a powder, washed with hot water, DMF and acetone, and dried in a vacuum oven.

Synthesis of Ag@TpBpy

To an aqueous suspension of TpBpy (10 mL, 6 mg mL^{-1}), the $AgNO_3$ aqueous solution (10 mL, 8.8 mmol L^{-1}) was added. The mixture was stirred at room temperature in the dark for 30 min. The solid ($AgNO_3$@TpBpy) was filtered out, washed with water and acetone, and dried in a vacuum oven. $AgNO_3$@TpBpy was redispersed in water (10 mL), and hydrazine hydrate (85%, 500 μL) was added. After stirring for 30 min at room temperature, Ag@TpBpy was filtered, washed with water and acetone, and dried in a vacuum oven.

Conflicts of interest

There are no conflicts to declare.

Acknowledgements

This research was supported by the National Natural Science Foundation of China (Grant No. 21773070 and 21971069).

References

1. L.-J. Zhou, W. Sun, N.-N. Yang, P. Li, T. Gong, W.-J. Sun, Q. Sui and E.-Q. Gao, *ChemSusChem*, 2019, **12**, 2202-2210.
2. E. A. Quadrelli and G. Centi, *ChemSusChem*, 2011, **4**, 1179-1181.
3. Q.-W. Song, Z.-H. Zhou and L.-N. He, *Green Chem.*, 2017, **19**, 3707-3728.
4. M. He, Y. Sun and B. Han, *Angew. Chem., Int. Ed.*, 2013, **52**, 9620-9633.
5. Q. Liu, L. Wu, R. Jackstell and M. Beller, *Nat. Commun.*, 2015, **6**, 5933.
6. A. J. Kamphuis, F. Picchioni and P. P. Pescarmona, *Green Chem.*, 2019, **21**, 406-448.
7. W.-S. Liu, L.-J. Zhou, G. Li, S.-L. Yang and E.-Q. Gao, *ACS Sustainable Chem. Eng.*, 2021, **9**, 1880-1890.
8. S.-L. Hou, J. Dong and B. Zhao, *Adv. Mater.*, 2020, **32**, 1806163.
9. Y. Yuan, C. Chen, C. Zeng, B. Mousavi, S. Chaemchuen and F. Verpoort, *ChemCatChem*, 2017, **9**, 882-887.
10. H. Cheng, B. Zhao, Y. Yao and C. Lu, *Green Chem.*, 2015, **17**, 1675-1682.
11. G. Bresciani, F. Marchetti and G. Pampaloni, *New J. Chem.*, 2019, **43**, 10821-10825.
12. M. Poliakoff, W. Leitner and E. S. Streng, *Faraday Discuss.*, 2015, **183**, 9-17.
13. C.-X. Guo, B. Yu, J.-N. Xie and L.-N. He, *Green Chem.*, 2015, **17**, 474-479.
14. B. Pieber, T. Glasnov and C. O. Kappe, *RSC Adv.*, 2014, **4**, 13430-13433.
15. A. Polyzos, M. O'Brien, T. P. Petersen, I. R. Baxendale and S. V. Ley, *Angew. Chem., Int. Ed.*, 2011, **50**, 1190-1193.
16. D. Yu and Y. Zhang, *Green Chem.*, 2011, **13**, 1275-1279.
17. F.-W. Li, Q.-L. Suo, H.-L. Hong, N. Zhu, Y.-Q. Wang and L.-M. Han, *Tetrahedron Lett.*, 2014, **55**, 3878-3880.
18. X. Wang, Y. N. Lim, C. Lee, H.-Y. Jang and B. Y. Lee, *Eur. J. Org. Chem.*, 2013, **2013**, 1867-1871.
19. S. Ghosh, A. Ghosh, S. Riyajuddin, S. Sarkar, A. H. Chowdhury, K. Ghosh and S. M. Islam, *ChemCatChem*, 2020, **12**, 1055-1067.
20. Z. Wu, L. Sun, Q. Liu, X. Yang, X. Ye, Y. Hu and Y. Huang, *Green Chem.*, 2017, **19**, 2080-2085.
21. D. J. Shah, A. S. Sharma, A. P. Shah, V. S. Sharma, M. Athar and J. Y. Soni, *New J. Chem.*, 2019, **43**, 8669-8676.
22. F. Manjolinho, M. Arndt, K. Goossen and L. J. Goossen, *ACS Catal.*, 2012, **2**, 2014-2021.
23. D. Yu and Y. Zhang, *Proc. Natl. Acad. Sci. U. S. A.*, 2010, **107**, 20184-20189.
24. P. Yang, S. Zuo, F. Zhang, B. Yu, S. Guo, X. Yu, Y. Zhao, J. Zhang and Z. Liu, *Ind. Eng. Chem. Res.*, 2020, **59**, 7327-7335.
25. W. Zhang, Y. Mei, X. Huang, P. Wu, H. Wu and M. He, *ACS Appl. Mater. Interfaces*, 2019, **11**, 44241-44248.
26. W.-J. Sun and E.-Q. Gao, *Appl. Catal., A*, 2019, **569**, 110-116.
27. A. H. Chowdhury, U. Kayal, I. H. Chowdhury, S. Ghosh and S. M. Islam, *ChemistrySelect*, 2019, **4**, 1069-1077.
28. B. Yu, P. Yang, X. Gao, Z. Yang, Y. Zhao, H. Zhang and Z. Liu, *Sci. China: Chem.*, 2018, **61**, 449-456.
29. B. Yu, P. Yang, X. Gao, Z. Z. Yang, Y. F. Zhao, H. Y. Zhang and Z. M. Liu, *New J. Chem.*, 2017, **41**, 9250-9255.
30. K. Geng, T. He, R. Liu, K. T. Tan, Z. Li, S. Tao, Y. Gong, Q. Jiang and D. Jiang, *Chem. Rev.*, 2020, **120**, 8814-8933.
31. S. Kandambeth, K. Dey and R. Banerjee, *J. Am. Chem. Soc.*, 2019, **141**, 1807-1822.
32. A. P. Cote, A. I. Benin, N. W. Ockwig, M. O'Keeffe, A. J. Matzger and O. M. Yaghi, *Science*, 2005, **310**, 1166-1170.
33. Q. Sun, B. Aguila, J. Perman, L. D. Earl, C. W. Abney, Y. Cheng, H. Wei, N. Nguyen, L. Wojtas and S. Ma, *J. Am. Chem. Soc.*, 2017, **139**, 2786-2793.
34. X. Wang, L. Chen, S. Y. Chong, M. A. Little, Y. Wu, W.-H. Zhu, R. Clowes, Y. Yan, M. A. Zwijnenburg, R. S. Sprick and A. I. Cooper, *Nat. Chem.*, 2018, **10**, 1180-1189.
35. Q. Xu, H. Zhang, Y. Guo, J. Qian, S. Yang, D. Luo, P. Gao, D. Wu, X. Li, Z. Jiang and Y. Sun, *Small*, 2019, **15**, 1905363.
36. Z. Fu, X. Wang, A. M. Gardner, X. Wang, S. Y. Chong, G. Neri, A. J. Cowan, L. Liu, X. Li, A. Vogel, R. Clowes, M. Bilton, L. Chen, R. S. Sprick and A. I. Cooper, *Chem. Sci.*, 2020, **11**, 543-550.
37. W. K. Haug, E. R. Wolfson, B. T. Morman, C. M. Thomas and P. L. McGrier, *J. Am. Chem. Soc.*, 2020, **142**, 5521-5525.
38. X. Zhao, P. Pachfule, S. Li, T. Langenhahn, M. Ye, C. Schlesiger, S. Praetz, J. Schmidt and A. Thomas, *J. Am. Chem. Soc.*, 2019, **141**, 6623-6630.
39. Y. Zhi, Z. Wang, H.-L. Zhang and Q. Zhang, *Small*, 2020, **16**, 2001070.
40. J. Guo and D. Jiang, *ACS Cent. Sci.*, 2020, **6**, 869-879.
41. W. Zhong, R. Sa, L. Li, Y. He, L. Li, J. Bi, Z. Zhuang, Y. Yu and Z. Zou, *J. Am. Chem. Soc.*, 2019, **141**, 7615-7621.
42. H.-J. Zhu, M. Lu, Y.-R. Wang, S.-J. Yao, M. Zhang, Y.-H. Kan, J. Liu, Y. Chen, S.-L. Li and Y.-Q. Lan, *Nat. Commun.*, 2020, **11**, 497.
43. P. Puthiaraj, H. S. Kim, K. Yu and W.-S. Ahn, *Microporous Mesoporous Mater.*, 2020, **297**, 110011.
44. Q.-Q. Dang, C.-Y. Liu, X.-M. Wang and X.-M. Zhang, *ACS Appl. Mater. Interfaces*, 2018, **10**, 27972-27978.
45. X. Lan, C. Du, L. Cao, T. She, Y. Li and G. Bai, *ACS Appl. Mater. Interfaces*, 2018, **10**, 38953-38962.
46. R. Bu, L. Zhang, L.-L. Gao, W.-J. Sun, S.-L. Yang and E.-Q. Gao, *Mol. Catal.*, 2021, **499**, 111319.
47. S. Karak, S. Kandambeth, B. P. Biswal, H. S. Sasmal, S. Kumar, P. Pachfule and R. Banerjee, *J. Am. Chem. Soc.*, 2017, **139**, 1856-1862.
48. D. Chakraborty, P. Shekhar, H. D. Singh, R. Kushwaha, C. P. Vinod and R. Vaidhyanathan, *Chem. - Asian J.*, 2019, **14**, 4767-4773.
49. N. Salam, S. K. Kundu, R. A. Molla, P. Mondal, A. Bhaumik and S. M. Islam, *RSC Adv.*, 2014, **4**, 47593-47604.
50. J. J. Jarju, A. M. Lavender, B. Espina, V. Romero and L. M. Salonen, *Molecules*, 2020, **25**.
51. L. Wang, H. Xu, Y. Qiu, X. Liu, W. Huang, N. Yan and Z. Qu, *J. Hazard. Mater.*, 2020, **389**, 121824.
52. M. Trivedi, G. Singh, A. Kumar and N. P. Rath, *Dalton Trans.*, 2015, **44**, 20874-20882.
53. M. Lohrie and W. Knoche, *J. Am. Chem. Soc.*, 1993, **115**, 919-924.
54. J. M. Sanchez-Ruiz, J. Llor and M. Cortijo, *J. Chem. Soc., Perkin Trans. 2*, 1984, 2047-2051.
55. F. G. Bordwell, G. E. Drucker, N. H. Andersen and A. D. Denniston, *J. Am. Chem. Soc.*, 1986, **108**, 7310-7313.
56. R. Schmitt, *Journal für Praktische Chemie*, 1885, **31**, 397-411.
57. Y. Kosugi, M. A. Rahim, K. Takahashi, Y. Imaoka and M. Kitayama, *Appl. Organomet. Chem.*, 2000, **14**, 841-843.
58. Z. Markovic, S. Markovic, N. Manojlovic and J. Predojevic-Simovic, *J. Chem. Inf. Model.*, 2007, **47**, 1520-1525.
59. C. Wang, H. Luo, H. Li, X. Zhu, B. Yu and S. Dai, *Chem. - Eur. J.*, 2012, **18**, 2153-2160.